Impact of synoptic meteorological conditions on air quality in three different case studies in Rome, Italy

Annalisa Di Bernardino[1,*], Anna Maria Iannarelli[2], Stefano Casadio[2], Cinzia Perrino[3], Francesca Barnaba[4], Luca Tofful[3], Monica Campanelli[4], Luca Di Liberto[4], Gabriele Mevi[2], Anna Maria Siani[1] and Marco Cacciani[1]

[1] Physics Department, Sapienza University, Rome, Italy
[2] SERCO SpA, Frascati, Rome, Italy;
[3] National Research Council of Italy, Institute of Atmospheric Pollution Research (CNR-IIA), Monterotondo st., Rome, Italy;
[4] National Research Council of Italy, Institute of Atmospheric Sciences and Climate (CNR-ISAC), Rome, Italy;
***** Correspondence: annalisa.dibernardino@uniroma1.it

Keywords: particulate matter, air quality, atmospheric pollutant, synoptic circulation, urban environment

Highlights:

- PM10 concentration have been studied in urban and rural air quality stations
- Air quality improves when northerly, synoptic winds persist for at least 24 hours
- During thermal inversions, the change in weather conditions can improve air quality
- During Saharan dust outbreaks, PM10 content increases in urban and rural stations
- Traffic blocks should be defined in advance if strong inversion events are expected

Abstract: This study analyses the influence of synoptic weather conditions on atmospheric particulate matter concentration and composition during an intensive measurement campaign, performed in the urban area of Rome (Italy) in winter 2017. To evaluate the effect of local particulate sources, data from several urban and rural ground-based air quality stations were considered. The analysis involved the following atmospheric parameters: wind speed and direction near the ground, air temperature, specific humidity, height and evolution of the mixing layer. Furthermore, the daily variability of aerosol optical depth, tropospheric and near-surface nitrogen dioxide amounts were investigated. Results show that the natural removal of particulate matter is favoured by intense, continental winds. Contrariwise, when persistent thermal inversion occurs, pollutant dispersion is very limited and high concentrations are recorded by urban stations. Finally, in the case of Saharan dust outbreaks, an increase in the particulate content in both urban and rural stations is notable. Consequently, specific measurements aimed at improving air quality in urban environments should be planned according to synoptic weather and aerosol forecasts. This keeps valid in specific conditions of long-range transport of desert dust particles when the natural contribution could exceed that of pollutants from anthropogenic emissions.

1. Introduction

Air pollution is one of the major problems affecting urban areas, causing harmful effects on human health (Kim et al., 2015; Pope et al., 2002) and reducing visibility (Jayaratne et al., 2015). It also influences climate as it alters Earth's radiative balance in different ways, depending on its composition (Zhao et al., 2020).

European and Italian legislation include PM_{10}, i.e. the fraction of particle matters with an aerodynamic diameter smaller than 10 μm, among the target pollutants for assessing air quality. Specifically, Directive 1999/30/EC (EU, 1999) introduced two different limits for protecting human

health: by 1 January 2005, the daily-average concentration of PM_{10} threshold (i.e. 50 $\mu g/m^3$) can be exceeded at most 35 days in a calendar year, while the annual average concentration should not be higher than 40 $\mu g/m^3$. The Directive defines a second stage in which the limit of 50 $\mu g/m^3$ is not to be exceeded more than seven times per year, while the annual average threshold is lowered to 20 $\mu g/m^3$. Although the update should have started on January 1, 2010, it actually has not yet become effective and the legal limits are still those defined in the first stage. Moreover, the European Air Quality Directive 2008/50/EC (EU, 2008) establishes the legal limits for various atmospheric pollutants, including NO_2. For the latter, the reference thresholds are 200 $\mu g/m^3$ (as hourly average, not to be exceeded on more than 18 times a calendar year) and 40 $\mu g/m^3$ as annual average.

Even if EU air quality policy has led to significant reduction in harmful pollutant concentrations, fine particulate matter (PM_{10} and $PM_{2.5}$), nitrogen oxides (e.g. NO_2) and ozone (O_3) continue to represent serious health risks. In fact, the WHO air quality guidelines (World Health Organization, 2000) indicate an annual average threshold limit of 20 $\mu g/m^3$ for PM_{10} and 10 $\mu g/m^3$ for $PM_{2.5}$ as the harmful effects of PM on health are still important at concentrations below the daily average limits imposed by EU. These limits are largely exceeded in Europe (and Italy).

Local governments can adopt measures in order to reduce atmospheric pollution by favouring low-emission technologies, creating limited road traffic areas or, in extrema ratio, establishing partial or total traffic blocking. Nevertheless, due to different and often concurring reasons, these actions do not always cause the desired effect of reducing the atmospheric particulate matter concentration (Davis, 2008; Viard and Fu, 2015; Campanelli et al., 2021).

The air pollution management is particularly complex in large metropolitan areas, where the local micrometeorological conditions, driven by the urban canopy geometric and thermodynamic characteristics, further complicate the picture also giving rise to the well-known phenomenon of the Urban Heat Island (UHI) (Oke, 1973). In fact, air quality is particularly degraded due to the presence of tall buildings that shield intense wind and induce air stagnation, with the consequent reduction of pollutants dispersion (Di Bernardino et al., 2018; Barbano et al., 2020). For this reason, pollutants emitted near the ground remain trapped at the pedestrian level, increasing the health damages, especially in the case of specific meteorological conditions, such as thermal inversion or very stable stratification (Palmieri et al., 2008).

In the last decades, several studies demonstrated the strong correlation between PM concentrations and synoptic weather conditions (Rojas et al., 2020; Hassan et al., 2020; Baltaci et al., 2020). E.g., high-level PM_{10} episodes were associated with four distinct meteorological synoptic patterns in an industrial and highly polluted region of Greece: highest concentrations corresponded to stagnant conditions, while only few events were associated with high wind speed days (Triantafyllou, 2001). In Italy, Fortelli et al. (2008) studied events of high PM_{10} levels in the metropolitan area of Naples, Italy. Naples is a coastal city and, although it is smaller than Rome, the geographic position and the local scale weather conditions are comparable. They investigated the relationship between synoptic/local meteorological patterns and PM_{10} air pollution levels, finding that values exceeded the legal threshold during the winter mainly in the case of weak wind intensity, thermal inversion and with no significant rainfall for at least 7 days.

Natural aerosols also contribute to atmospheric particulate matter. In the area under investigation, the impact of Saharan dust outbreaks on ambient PM_{10} concentrations has been shown to be important (Pey et al., 2013; Barnaba et al., 2017) and, in some episodes, comparable or even higher with respect to the anthropogenic one. In addition, as reported by (Gobbi et al., 2019), in Rome more than 30% of the days when PM_{10} levels exceed the legal thresholds are characterized by a significant presence of desert dust.

The influence of synoptic circulation and other planetary boundary layer (PBL) dynamic characteristics on PM_{10} concentrations and UHI intensity (defined as the temperature difference between urban area and rural surroundings (Martin-Vide et al., 2015)) was evaluated by He et al., (2013) using MM5 model to study wintertime air pollution in Changsha, one of the most polluted cities in China. As expected, they found a reduction of PM_{10} concentration (<120 $\mu g/m^3$) and UHI

intensity (about -1 °C) when high wind speed (>1.8 m/s) and high mixing layer height (MLH) (>900 m) occur. Contrariwise, high PM_{10} concentrations (>180 $\mu g/m^3$) and high UHI intensity (2 °C) were associated with weak mixing layer height (<300 m).

It is evident that several parameters must be considered to comprehensively analyse the dynamic of atmospheric pollutant dispersion in the urban environment and to investigate the contaminants concentration in the surface layer. A detailed knowledge of the mesoscale circulation, which results from the combination of synoptic weather patterns and local flows induced by the complex geometry, is required. Additionally, the analysis must also include ground temperature and specific humidity, as their variation can affect the pollution levels (Elminir, 2005), wind speed and direction (which in turn greatly affect the horizontal and vertical dispersion (Cantelli et al., 2015)), and the MLH and its daily evolution (Su et al., 2018), which determine the layer of the atmosphere near the ground in which the pollutants are dispersed.

In this work, we focused on three specific events occurred in the Rome area (Italy) during winter 2017, when the intensive campaign of the project "Integrated Evaluation of Indoor Particulate Exposure" (VIEPI) (Pelliccioni et al., 2020) was carried out at the Atmospheric Physics Laboratory (hereinafter, APL station), located at the Physics Department of the Sapienza University of Rome. The three events were chosen based on the PM_{10} level recorded in different air quality stations, both in the urban and rural areas around Rome and were selected as representative of as many paradigmatic categories of meteorological conditions in the Rome area. The first episode (27 November), was characterized by very low concentrations of PM_{10} all over the city and can be considered as an example of "optimal" weather and ventilation conditions favouring pollutants dispersion. In the other two events, registered respectively from 4 to 7 December and on 12 December, urban and rural air quality stations measured daily mean concentrations of PM_{10} above the legal limit, even if the local and synoptic conditions were quite different in the two cases. To deepen the investigation of pollutants properties near the ground and in the lower atmosphere, in addition to the average daily concentration and composition of PM_{10}, also the trend of the aerosol optical depth (AOD) at 500 nm, the near-surface and tropospheric amounts of nitrogen dioxide (NO_2) were analysed. In fact, the health effects of PM_{10} and NO_2 have been widely investigated (Hart et al., 2009; Weinmayr et al., 2010), also associating long-term exposure to increased mortality rates (Heinrich et al., 2013).

The goal of this work is the evaluation of the influence of synoptic and local scale weather conditions on the daily average concentration of PM_{10} in an urban environment, focusing on the impact of anthropogenic components and natural sources. The proposed approach paves the way to long-term time series analyses and for the creation of a coherent climatology, which may be used in risk assessment and prevention policy for the mitigation of atmospheric pollution and in any future health policy.

The paper is structured as follows: Section 2 presents the measurement site. Section 3 describes the in-situ campaign framework, the instruments and the data used in this study. In Section 4, the main results are presented and discussed. In Section 5, conclusions and possible outlooks are depicted.

2. Site description

The Physics Department of the Sapienza University of Rome represents a favourable site for atmospheric studies thanks to its central position in the city of Rome, in a morphologically heterogeneous area, surrounded by buildings with complex geometries and different heights. The location is also useful for air quality studies as both the aerosol contribution due to local emissions and transport from distant regions can be explored (Ciardini et al., 2012; Campanelli et al., 2019; Mevi et al., 2021).

Rome is a coastal city, located about 27 km inland from the Tyrrhenian coast. The atmospheric circulation is strictly connected to the orography, with the alternation of two prevailing patterns due to the sea/land breeze regime (Di Bernardino et al., 2020). During the night, the wind blows mainly

from North North-East due to the drainage flow through the Tiber Valley while, during daytime, the sea breeze blows essentially from West South-West. The breeze regime is experienced throughout the year, depending on the synoptic and microscale weather conditions. During summer, i.e. when the different heat capacity of sea and land gives rise to significant temperature gradients that permit the penetration of the breeze front also in the inner metropolitan region (Cenedese et al., 2000), the breeze intensity increases and its occurrence is much more frequent (Petenko et al., 2011).

In the urban area of Rome, the main economic activities are services and transports, while emissions from industries are rather low as there are no highly industrialized areas near the city (Cattani et al., 2010). As a matter of fact, the concentration of airborne pollutants is highly influenced by the advection and medium-long range transport of Saharan dust (Gobbi et al., 2007; Gobbi et al., 2019), with maxima loads during spring and summer and minima in winter (Chester et al., 1984; Barnaba et al., 2011), by the breeze that carries high concentrations of marine aerosol into the hinterland (Perrino et al., 2009) and by fires (Barnaba et al., 2011; Perrino et al., 2019), i.e. by natural phenomena driven by the synoptic or local scale weather conditions. Pollution problems occur more frequently during winter, when there can be the concomitance of stable atmospheric conditions, low convection, thermal inversion, absent or low sea breeze and high anthropic emissions. In 2008, Perrino et al. analysed both concentration and chemical composition of PM_{10} from urban and rural air quality monitoring stations in Rome. Their outcomes showed an increase in PM_{10} concentration at the traffic stations mainly due to the increase of elemental carbon and dust resuspension. Instead, a link between the daily variation of the PM_{10} concentration and the dilution properties of the lower atmosphere has been found. It results in a net increase of PM_{10} during atmospheric stability events and low PM_{10} values during advection of continental and marine air. Moreover, recent epidemiological studies (Michelozzi et al., 2000; Avino et al., 2004) have shown statistically significant correlations between elevated levels of particulate matter in Rome and cardiopulmonary diseases and hence mortality, showing that a 10 $\mu g/m^3$ increase in PM_{10} concentration causes a 1.1% increase in mortality due to respiratory illnesses.

3. Instrumentation

From November 2016 to November 2019, the Physics Department of the Sapienza University of Rome was the main location of the VIEPI project experimental campaigns. The primary objective of this project was the evaluation of indoor air quality and the exposure to particulate matter of humans in workplaces (details in Pelliccioni et al., 2020). In this framework, several research teams collaborated to carry out extensive and intensive in-situ campaigns concerning atmospheric, micrometeorological, physical and chemical parameters to exhaustively analyse the correlation between outdoor and indoor PM concentrations.

The APL station hosts on the rooftop of the Physics Department a great number of atmospheric remote sensing instruments and, since 2017, it represents the urban component of the remote sensing measurement super-site BAQUNIN (Boundary-layer Air Quality-analysis Using Network of Instruments, in-depth details about instrumentation and site can be found at https://www.baqunin.eu/).

In addition, this study was extended and deepened using data from stations located in the urban area of Rome and belonging to other national and international networks. Climate Network and OMD Foundation (Fondazione Osservatorio Meteorologico Milano Duomo, https://www.fondazioneomd.it/) gave surface air temperature, wind speed and relative humidity. The air quality monitoring network managed by Regional Environmental Protection Agency of Lazio region (ARPA Lazio, http://www.arpalazio.gov.it/ambiente/aria/) provided the daily-averaged concentrations of PM_{10} for several urban and rural stations. The Italian Automated Lidar-CEilometer (ALC) network (ALICEnet, www.alice-net.eu) provided information regarding the daily evolution of the MLH all over the country in partnership with other Italian research institutions and environmental agencies, and is part of the European network E-Profile coordinated by EUMETSAT (https://e-profile.eu). Moreover, the Pandonia Global Network (PGN, https://www.pandonia-global-network.org/) provided measurements of tropospheric and near-surface NO_2 amounts, while the

analysis of the AOD was carried out thanks to data from the international network AERONET-EUROPE (https://aeronet.gsfc.nasa.gov/). Both AERONET and PGN instruments operating at APL are part of the BAQUNIN super-site.

In the following, the main characteristics of the instruments involved in this work are briefly presented.

The Doppler SODAR (Sonic Detection and Ranging), part of the BAQUNIN super-site, operated continuously providing information on atmospheric thermal turbulence up to a maximum altitude of 230 m.a.s.l. with 1 Hz pulse repetition rate. The three-axial, monostatic configuration consists of a vertical antenna and two antennas tilted 20° from the zenith, pointing North and East, that emit simultaneously sound bursts of 0.1 s duration, with central frequencies of 4450.75, 4650.75, 4840.75 Hz. The instantaneous measurements were averaged over of 10-minute time intervals, obtaining vertical profiles of horizontal wind speed and wind direction (Mastrantonio and Fiocco, 1982). Since the focus is on anemological conditions near the ground, in this paper the wind velocity and direction at about 11 meters from the rooftop level (which is the first SODAR range gate not affected by electro-acoustic transducer membrane ringing and close to the rooftop of the building) are plotted. Details regarding the estimated uncertainties of U and θ can be found in Casasanta et al. (2020).

The Pandora 2S Sun-Moon spectrometer (LuftBlick, Innsbruck, Austria) is part of the PGN (Cede et al., 2019). Working in a wide spectral range (290-900 nm), PGN measurements allowed for estimates the atmospheric content of a number of trace gases, including tropospheric and near-surface amount of NO_2 by means of direct and diffuse solar radiation measurements (Spinei et al., 2020). The associated uncertainties were 0.03 DU and 3.60 ppb for tropospheric and quasi-surface NO_2 amounts, respectively (Cede, 2019).

The Cimel CE318-T Sun-photometer (Cimel Electronique, Paris, France) belonging to the AERONET-EUROPE network (Giles et al., 2017), performed measurement of direct and diffuse solar radiation at different wavelengths for the evaluation of AOD with a time resolution of about 10 minutes and an uncertainty of about 1-2% (Sinyuk et al., 2020)

The values of air temperature (T), wind speed (U) and relative humidity (used for the calculation of specific humidity using the Magnus–Tetens equation (Tetens, 1930)) at the rooftop of the APL building were obtained from the ground-based meteorological station (Vaisala Weather Transmitter WXT520, Vaisala, Helsinki, Finland) belonging to Climate Network. All data had a temporal resolution of 1 minute. The accuracy was ±0.3 °C for T (for sensor at 20 °C), ±3 % for U (with wind speed of 10 m/s) and ±3 % for relative humidity (within the range 0-90 %).

The daily-averaged concentrations of PM_{10} were obtained by selected ground-based air quality stations of the ARPA Lazio monitoring network. In Table 1, the main information about those stations are summarized: Magna Grecia (MG) and Francia (FR) are classified as urban traffic, as they are located on the sidewalk of highly trafficked streets; Cinecittà (CI) is considered as urban background station, even if it is it installed on a secondary road but close to one of the main urban streets, Villa Ada (VA) is inside a park and, therefore, is considered an urban background. Finally, the Castel di Guido (CG) station was chosen as a rural background, being located outside the city centre of Rome. Figure 1 shows the location of the selected stations. The PM_{10} average concentrations were routinely collected using a SWAM 5a Dual Channel Monitor (FAI Instruments, Fonte Nuova, Rome, Italy) in FR and VA stations, a SWAMDC (FAI Instruments, Fonte Nuova, Rome, Italy) in CI and CG and a MP101M (Envea, Verano Brianza, Monza Brianza, Italy) at MG. The analysis technique was based on the β attenuation methodology (Macias and Husar, 1976), which permitted an uncertainty on the mass measurement of 10 μg.

PM_{10} concentration was also measured at APL station using a β attenuation SWAM 5a Dual Channel Monitor. The two channels of the instrument were equipped with Teflon and quartz filters. After sampling, Teflon filters were analysed by energy-dispersion X-ray fluorescence (XRF; XEPOS, Spectro Analytical Instruments, Kleve, Germany) for Si, Al, Fe, Na, K, Mg, Ca and minor elements. Then, they were extracted in deionized water and analysed for ions (chloride, nitrate, sulfate, sodium, potassium, ammonium, magnesium, calcium) by ion chromatography (IC; ICS1000, Dionex Co.,

Sunnyvale, CA, USA). Quartz filters were analysed for elemental and organic carbon by thermo-optical analysis (OCEC Carbon Aerosol Analyser, Sunset Laboratory, Tigard, OR, USA; NIOSH–QUARTZ temperature protocol).

Table 1. Information on the air quality stations managed by ARPA Lazio and, in the last row, on Atmospheric Physics Laboratory station.

Station	Station ID	Latitude	Longitude	Altitude (m.a.s.l.)	Environment
Magna Grecia	MG	41.883	12.509	49	Urban traffic
Francia	FR	41.947	12.469	43	Urban traffic
Cinecittà	CI	41.858	12.569	53	Urban background
Villa Ada	VA	41.933	12.507	50	Urban background
Castel di Guido	CG	41.889	12.266	61	Rural background
Atmospheric Physics Laboratory	APL	41.902	12.516	75	Urban background

The main sources of PM were estimated as described in Farao et al. (2014). Briefly, soil contribution was calculated by summing the concentration of elements (as metal oxides) that are generally associated with mineral dust: Al, Si, Fe, the insoluble fractions of K, Mg and Ca (calculated as the difference between the XRF and the IC determinations), calcium and magnesium carbonate. Sea-salt contribution was calculated from the sum of soluble sodium and chloride, multiplied by 1.176 to consider minor sea-water components. Secondary inorganics (sulphate, nitrate and ammonium) were considered individually. Traffic contribution was calculated as the amount of elemental carbon (EC) plus the same amount multiplied by 1.1 to take into account organic species that condense from the exhausts gases and coat the surface of elemental carbon particles. The remaining amount of organic carbon (OC), multiplied by 1.8 to account for non-C atoms in the organic molecules, constituted the organics.

The Nimbus CHM15K (Lufft, Fellbach, Germany) ALCs running in ALICEnet are high-performance systems providing vertical profiles of aerosols and clouds in the first 15 km of the atmosphere with a temporal resolution of 30 seconds and a vertical resolution of 15 m. The ALC instrument used in this study is located in Rome downtown, on the roof of the ARPA Lazio headquarters (41.910 N, 12.497 E), quite close to the APL site (approximatively 2 km, light blue symbol in Figure 1). It is a modified prototypal version of the CHM15K system developed in the framework of the DIAPASON project (Dionisi et al., 2018) to measure particles depolarization and up to now is the only ALC in Europe with depolarization capabilities. As in the standard CHM15K instrument, the laser emits polarized pulses at 1064 nm (pulse rate of 5-7 kHz and pulse energy of 8 µJ) and the receiver employs an avalanche photo-diode detector, however in this polarization-sensitive version a second detector-chain is added to sense and store the cross-polarized atmospheric return. Inference of MLH by ALC data is typically performed exploiting the aerosol signal gradients at the top of the lowermost aerosol layer, evolving through turbulent mixing during the day (Haeffelin et al., 2012). This method is quite efficient in most cases, main exceptions being extremely clean conditions (too weak aerosol signal) or when locally generated aerosols mix with non-local particles advected in the lowermost atmosphere. Aerosol gradients within the atmospheric profile are well detectable using different numerical methods, so that identification of aerosol layers can be performed quite accurately exploiting the high vertical resolution of the instrument (15 m). Main inaccuracy of the MLH derived by ALC derives from the ‘layer attribution problem’, i.e., selection of the aerosol

layer corresponding to the mixing layer when multiple aerosol stratifications are detectable along the profile. This aspect is extensively discussed in Haeffelin et al. (2012), highlighting how the attribution of the aerosol gradient retrievals to the top of a stable layer or a residual layer or a convectively mixed-layer height is the most difficult task. In their assessment, they concluded that this process succeeds at 50–70% of the time during the day when compared to radiosonde retrievals.

Moreover, data from radio soundings (Vaisala Radiosode RS92-SGP, Vaisala, Helsinki, Finland) provided by Italian Air Force Meteorological Service/World Meteorological Organization (SMAM/WMO), collected every 12 hours (00:00 UTC and 12:00 UTC) at the Pratica di Mare military airport (WMO code:16245, ICAO code: LIRE, 41.670 N, 12.450 E), were used to study the vertical profiles of air temperature.

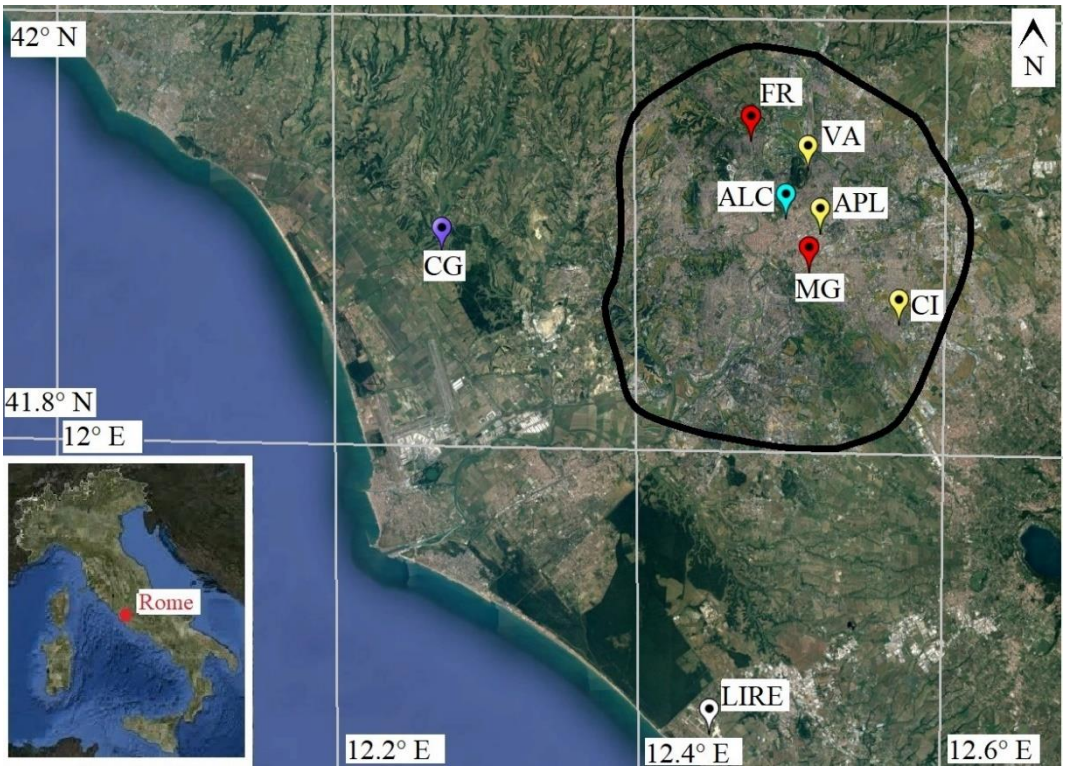

Figure 1. Location of Rome in central Italy and position of the air quality stations considered in the present study: traffic urban, urban background and rural stations are depicted in red, yellow and purple, respectively. Moreover, the ALC (light blue) and Pratica di Mare (LIRE) (white) sites are shown. Black line identifies the urban area of Rome. Source: Google Earth.

4. Results and discussion

In the winter period, the limit of PM_{10} concentration imposed by Directive 1999/30/EC for air pollution is often exceeded in Rome. The high concentrations, due to local emissions from vehicular traffic and domestic heating, superimpose to loadings from medium-to-long range advections.

Here, the period 17 November – 17 December 2017, belonging to the intensive winter campaign of the VIEPI project, was analysed. During that month, the synoptic-scale weather conditions were rather unstable, with the alternation of low-pressure systems descending from central Europe and high-pressure ridges over southern Italy and the central area of Mediterranean basin. In conjunction with the onset of low-pressure conditions, heavy rainfalls were recorded in the central region of Italy. In the examined period, the mean PM_{10} concentration measured at the APL

station was 28.4 µg/m^3 with a standard deviation of 13.3 µg/m^3. Airborne pollutants were composed on average by 22.3% (standard deviation 8%) of crustal materials, 9.7% (12.1%) of marine aerosols, 12.7% (4.1%) of secondary inorganic aerosols, 36.3% (12.1%) of organic aerosols and 19% (8.2%) of primary anthropogenic aerosols. Although located on a secondary road and classified as urban background station (see Table 1), CI is strongly affected by the intense traffic that occurs in the neighbouring streets. This justifies the high PM_{10} concentration values, which are comparable to those measured at MG and FR, classified as traffic stations.

Figure 2 shows the daily average concentrations of PM_{10} measured in the urban and rural air quality stations. Figure 3a presents the time record of horizontal wind speed (U) and wind direction (θ) measured by the SODAR at about 11 meters from the rooftop level (first range gate not affected by electro-acoustic transducer membrane ringing). Figure 3b shows the air temperature (T) as measured by the ground-based meteorological station installed at the rooftop of APL site during the winter campaign, while Figure 3c depicts the time record of the specific humidity (q) computed using measures from the same meteorological station.

During the period examined, the concentration of PM_{10} shows behaviours worthy of attention and discussion in the three events highlighted by grey bands in Figure 2. This work focuses on these three episodes, which could be useful to understand how the synergic effect of the synoptic circulation pattern and the ground-level weather conditions affects the pollutants dispersion in an urban environment. In order to deeply understand the weather conditions during the investigated periods, Figure 4 shows the vertical profiles of air temperature as measured by the radio soundings conducted at LIRE military airport at 00:00 UTC and 12:00 UTC. In Figure 5a, the 24-hours average chemical composition of particulate matters measured at APL station for the three episodes investigated is depicted while, in Figure 5b, the PM_{10} roses from the ground-based air quality stations for the three selected events are given.

The detailed discussion of the phenomena observable in Figures 2, 3, 4 and 5 is presented in the following subsections, focusing on the three cases under examination.

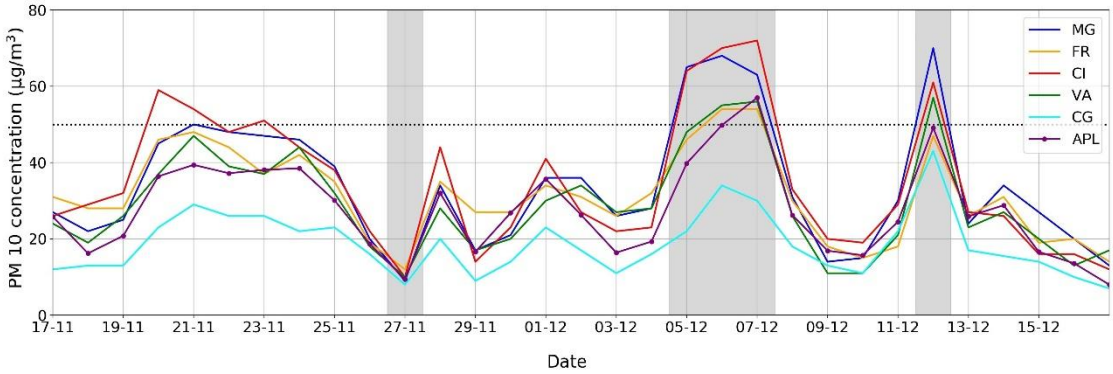

Figure 2. Daily average concentration of PM_{10} measured by five air quality stations (described in Table 1) belonging to ARPA Lazio network (lines) and by PM_{10} sampler located at APL station (marked line). The grey-shaded regions indicate the three events analysed in the present study.

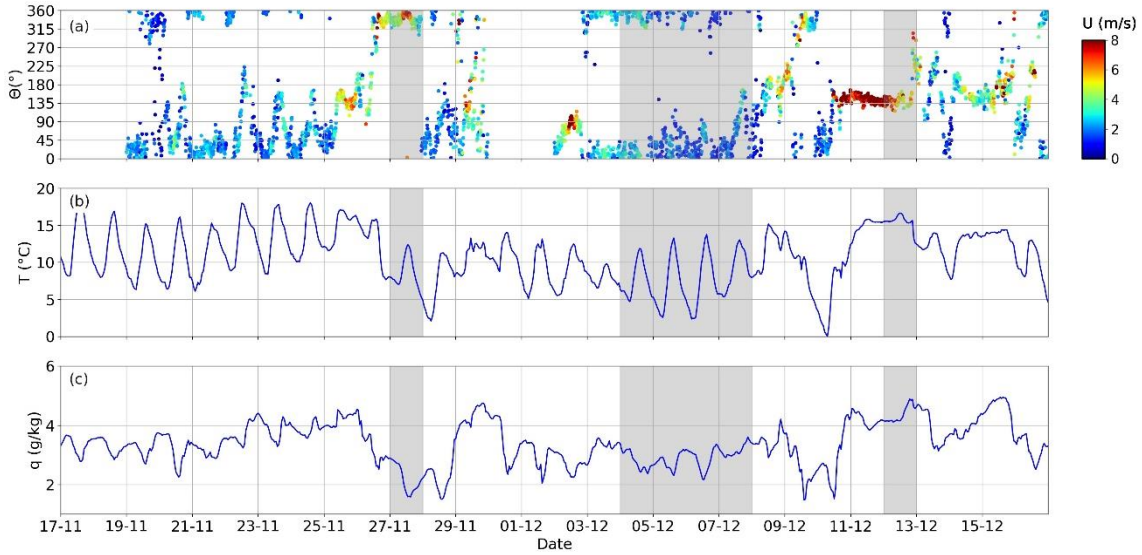

Figure 3. Temporal trend of meteorological parameters measured at APL: (a) wind speed and direction by SODAR at its first range gate, (b) air temperature and (c) specific humidity by ground-based meteorological station. Note that the specific humidity is not directly measured by it is computed following Tetens (1930). The grey-shaded regions indicate the three events analysed in the present study.

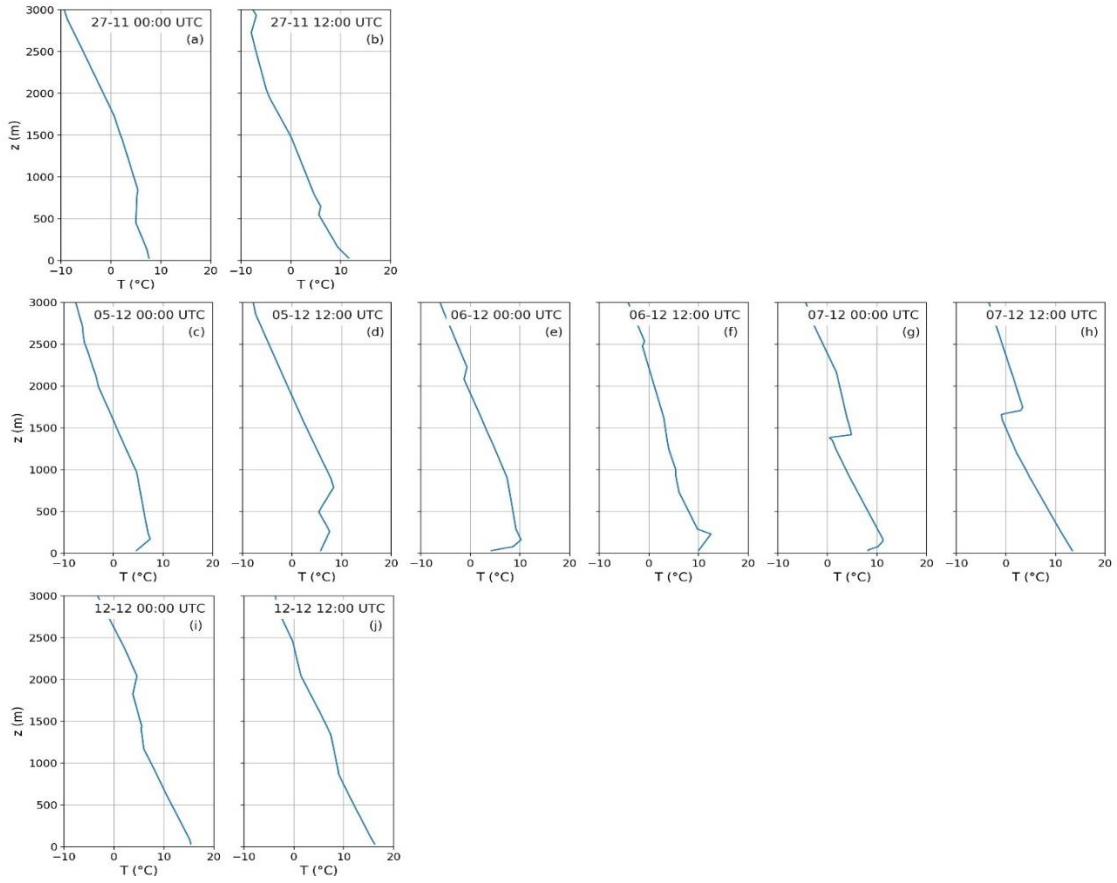

Figure 4: Vertical profiles of air temperature measured at LIRE airport at 00:00 UTC and 12:00 UTC for (a-b) case study #1, (c-h) case study #2 and (i-j) case study #3 discussed in the following subsections.

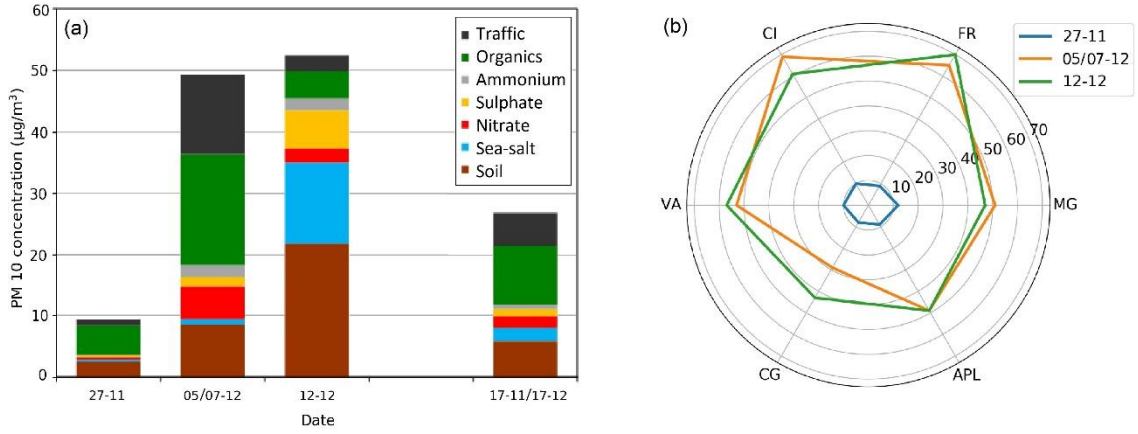

Figure 5. (a) Chemical composition of PM_{10} at APL station during the three considered events and mean composition during the study period. (b) Polar plot comparing the PM_{10} concentrations (plot radius, in $\mu g/m^3$) measured by the five air quality stations belonging to ARPA Lazio network during the investigated events.

4.1.Case study #1: 27 November 2017

The first attention-grabbing event occurred on 27 November. Figure 6a shows the map of the equipotential height contours at 850 hPa over central Europe at 12:00 UTC: a high-geopotential heights centre was located over the Atlantic Ocean, while a low-geopotential heights system was moving from Northern Europe to the Italian peninsula. Low-geopotential height on the Balkans indicates the presence of a cyclonic system, which determined northern sector synoptic winds over Italy. During the day, no significant changes in the circulation pattern were experienced.

As can be seen in Figure 6a, the synoptic conditions prevailed over local circulation patterns: near the ground, the SODAR measured wind blowing from the North North-West quadrant throughout the day, with wind velocity between 4 and 8 m/s (Figure 3a). Note that there was no day-to-night change in wind direction and that there was no breeze onset. Wind speed decreased closer to the ground: as shown in Figure 6b, the weather station recorded average wind speeds between 3 and 4 m/s, with peaks up to 8 m/s. The cold, northerly wind, typical of the winter season, caused a sharp decrease in air temperature (Figure 6c), which reached a maximum of 12.4 °C at 13:00 UTC and a minimum of 4.9 °C at 24:00 UTC. Because of the cold front, temperatures continued to decrease also during the following night up to 2 °C and no thermal inversion are measured by the Pratica di Mare radio soundings (Figure 4, panels a and b). As the wind came from the North North-West quadrant, the air was particularly dry, as evidenced by the q values (Figure 6d), which reached a minimum of 1.6 g/kg at 15:00 UTC. The MLH (Figure 6e), as derived by ceilometer measurements using the aerosol layer as tracer, reached the absolute daily maximum at 12:15 UTC (about 1250 m) and a relative maximum at 14:10 UTC (about 1200 m). Between the two maximum altitudes, the MLH decreased, with a minimum at 15:00 (about 820 m) likely due to increased wind (aerosol removal effect) in the upper levels of the PBL. The MLH reached during the day underlines the presence of high atmospheric turbulence, which favoured the pollutants dispersion. From 15:00 UTC onwards, as expected, the height of the MLH decreased, leading to the night stable layer.

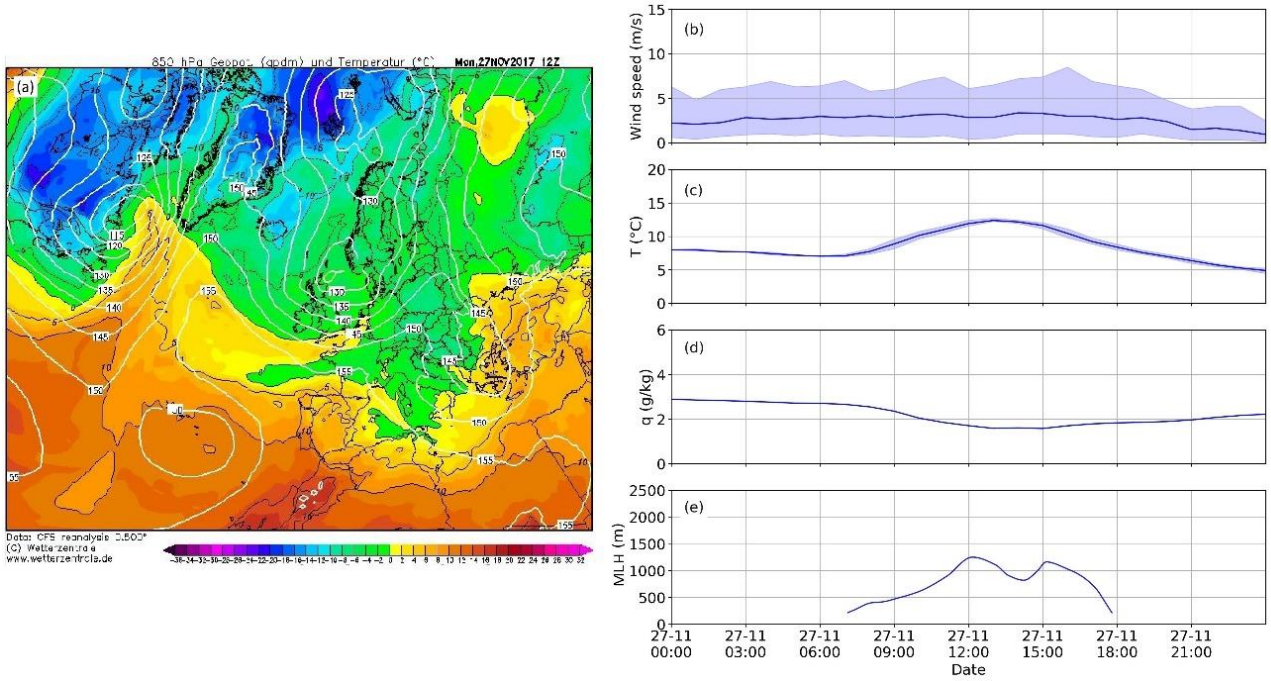

Figure 6. (a) Synoptic weather conditions on 27 November 2017 at 12:00 UTC from the Climate Forecast System (CFS) reanalysis. White contours refer to geopotential height at 850 hPa (in geopotential decametres). Colours show air temperature (°C) at sea level (source: https://www.wetterzentrale.de/). Trend of (b) wind speed, (c) air temperature (d) specific humidity as a function of the time of day provided by ground-based meteorological station at APL and (e) MLH from the ceilometer. Minimum and maximum values are depicted by filled regions.

As shown in Figures 2 and 5b, all the stations classified by ARPA Lazio network as urban traffic and urban background, measured particulate mass concentrations conform to the rural station of CG. The daily average concentration, considering all the five air quality stations, was 8.3 µg/m^3. The chemical composition of PM_{10} at APL station shows that the contribution of sea-salt, secondary inorganics (nitrate, sulphate and ammonium) and traffic were very low with respect to the average composition during the study period. During this clean air event, PM_{10} composition was dominated by organics (51%) and soil components (27%), that is, by natural sources. As the wind did not blow from the coast, the contribution of sea-salt was negligible. The rather high contribution of crustal particles was also confirmed by the ALC depolarization values in the lowermost levels (not shown).

In parallel with the analysis of PM_{10}, to complete the in-depth analysis, the temporal trend of AOD (Figure 7a), tropospheric (Figure 7b) and near-surface (Figure 7c) NO_2 amounts, mainly due to local emissions, were also analysed. Note that the range of the vertical axis in the tropospheric and near-surface NO_2 graphs have been adjusted to the concentration values measured in individual cases.

The AOD at 500 nm is very low, confirming the clean aerosol conditions through the entire atmospheric column. It increased in the early hours of the morning (from 7:10 to 9:00 UTC) passing from 0.05 to 0.07, and then settling on about 0.07. The data are only available until about 12:15 UTC as in the afternoon the presence of clouds did not allow the measurements. The tropospheric and near-surface NO_2 values were almost constant during the day and lower than the seasonal averages obtained at the same measurement site (Mevi et al., 2021). The daily average value of the tropospheric NO_2 column amount was quite low (0.2 DU) as well as the near-surface concentration (9.2 ppb), confirming that the advection of intense, northerly winds has caused the dispersion of pollutants both near the ground and within the PBL. The uncertainties are quite low, assuming

values between 0.01 DU and 0.1 DU and between 3 ppb and 10 ppb for tropospheric and near-surface NO_2, respectively.

As a matter of fact, the intense continental winds with no precipitation determined the advection of drier and cleaner air, which favoured the rapid horizontal dispersion of pollutants and the homogenization of air quality conditions in urban and rural areas. Also Fortelli et al. (2016) found PM levels typically below the limit of 50 µg/m^3 when the wind has an intensity greater than 4 m/s, which facilitates the dispersion of pollutants. As a result, this day represents the "optimal" case in terms of ventilation and dispersion, as all the pollutants emitted near the ground in the urban area were quickly dispersed.

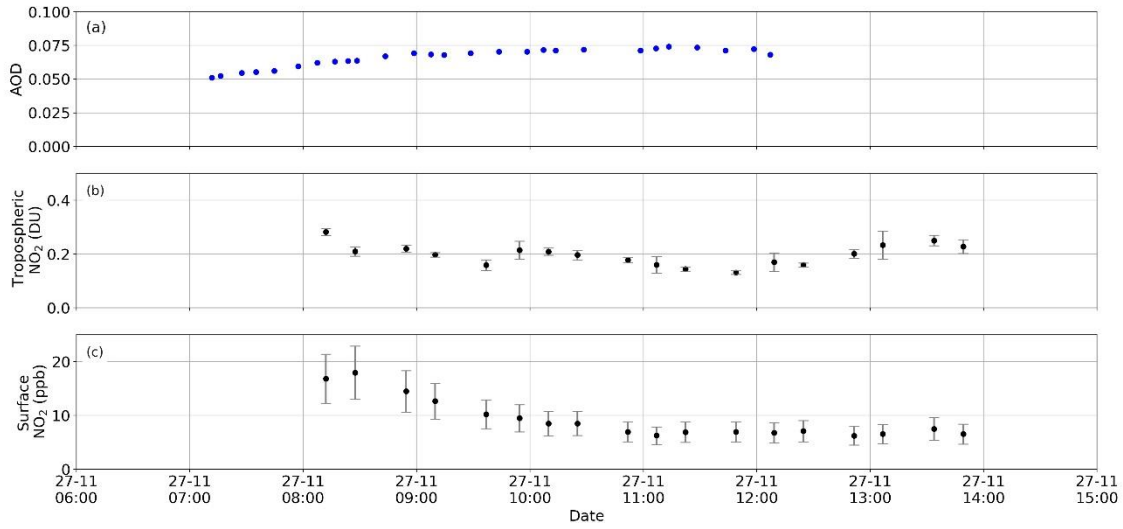

Figure 7. (a) Aerosol Optical Depth, (b) tropospheric and (c) near-surface amount of NO_2 measured at APL station as a function of the time of day on 27 November 2017. Vertical bars depict measurement errors. Note the different vertical scale in panels (b) and (c) with respect to the other events.

4.2.Case study #2: 5-7 December 2017

The second representative event took place from 5 to 7 December 2017. The geopotential height charts at 850 hPa pressure surface, referred at 12:00 UTC on the days examined, are presented in Figure 8 (panels a, b and c). During this period, a low-heights system was located north of the Scandinavian Peninsula with a trough shifting over the Balkan area and a high-heights system was present over the Iberian Peninsula and the western region of Mediterranean Basin. Moreover, on 7 December, a cyclonic system developed over the North Sea. This configuration governed the circulation in the Mediterranean area, causing air advection from mainland Europe to Italy. The weak gradient above Italy, due to the anticyclonic circulation on the Mediterranean, determined conditions of atmospheric stagnation with low-speed, northerly winds and without clouds and rainfalls. The ridge had weakened on 7 December, when the trough, located on the North Sea, rapidly moved towards the Italian Peninsula, causing atmospheric instability and heavy rainfalls.

The vertical air temperature profiles measured by radio soundings conducted in Pratica di Mare (Figure 4, panels from c to h) confirm that all the three days investigated were characterized by lasting surface temperature inversion conditions, i.e. a layer of atmosphere where temperature increases with height. This condition worsens air quality (Ji et al., 2012; Li et al., 2017) because a stable atmosphere stratification, typically occurring during thermal inversion, does not favour the development of the PBL. Consequently, vertical air movements, such as convection and turbulence, are mitigated, leading to the accumulation of particles and pollutants below the inversion layer

(Olofson et al., 2009). Near the ground, the wind came from North-North-East (Figure 3a) with velocities always lower than 4 m/s (Figure 8d). The condition of marked atmospheric stability did not allow the onset of the sea breeze and, only from 12:00 UTC on 7 December, there was a variation in wind direction (coming from East) even if with velocity lower than 2 m/s. Such low horizontal wind speed, in conjunction with the presence of thermal inversion layer, enhanced the stagnation of pollutants near the ground and, subsequently, the exceeding of the legal thresholds imposed on the 24-hours average concentrations of PM_{10}. It can be noticed in Figure 8e that air temperature had a strong diurnal excursion, oscillating between a minimum of 2.5 °C (4:00 UTC on 6 December) and a maximum of 14 °C (15:00 UTC on 6 December). The excursion decreased starting from 7 December, i.e. when the thermal inversion layer disappeared. The specific humidity (Figure 8f) did not show significant variations and it had minimum values in the daytime (2 g/kg at 12:00 UTC on 6 December) and maxima during the night (3.2 g/kg at 00:00 UTC on 6 December). The MLH, as shown in Figure 8g, reached lower values with respect to the event of 27 November, as expected in the case of thermal inversion and atmospheric stagnation. On December 5, the maximum MLH value of about 600 m was reached at 14:00 UTC. During the afternoon, the ALC-derived MLH further increased (reaching a maximum > 700 m at 17:15 UTC). Since that time, the MLH weakened very quickly, until 19:15 UTC (220 m). This afternoon effect can be a typical feature of ALC-derived MLH (Haeffelin et al., 2012). In fact, if after sunrise aerosols are lifted by convective mixing thus acting as very "good" tracers of the MLH, in the afternoon, when turbulence weakens due to decreasing sensible heat, the depth over which mixing occurs becomes shallower but the aerosols remain aloft, without evident subsidence. In these afternoon conditions, the strongest aerosol gradient corresponds to a "residual" aerosol layer aloft (Stull, 1988). On 6 December, the MLH was similar to the previous day with slightly higher values (maximum height of about 800 m reached around 16:00 UTC). Again, the transition to the stable boundary layer occurred sharply. On 7 December, unlike the previous days, the MLH developed quickly, reaching the maximum altitude of 1050 m at 13:30 UTC and remained well established until 18:00 UTC. The different behaviour of this day can be justified by observing the trend of the near-surface wind measured by the SODAR (Figure 3a): from 12:00 UTC onwards, in fact, the wind increased in intensity (from 2 to 4 m/s) and changed direction, blowing from the Southeast quadrant.

During the entire event, the FR station followed the VA station trend (Figure 5b), even if the former was located on a sidewalk and the latter in a park. This behaviour is linked to the wind direction measured near the ground: the FR air quality station is located along a road with North-South axis so, when the wind blows from North, as during this event (Figure 3a), the airflow is parallel to the road axis and the dispersion of ground-emitted pollutants is favoured. On 5 December, the concentration of airborne particles measured by all the stations analysed increased significantly (Figure 2): the growth was greater in the CI and MG stations, which measured an escalation of 178% and 132% compared to previous day, exceeding the legal PM_{10} daily threshold (average daily concentrations of 64 $\mu g/m^3$ and 65 $\mu g/m^3$, respectively). In the APL station, a very marked increase (about 125%) was also recorded, although the concentration remained below the legal limits (40 $\mu g/m^3$). On 6 and 7 December, all the stations recorded increasing PM_{10} concentrations and the law limit was exceeded in all urban stations. The PM_{10} concentrations recorded by APL were generally lower than urban stations, confirming the "filter" effect operated by the University Campus (the nearest urban road is located about 40 meters from the station) and allowing the station to be considered as urban background. Only on 7 December, in APL station the measured concentration exceeded the threshold imposed by law. On 8 December, i.e. when the synoptic weather conditions changed thanks to the movement of the cyclonic system over Italy, the concentration of PM_{10} rapidly decreased in all the stations, returning well below the threshold value. As shown by the polar plot in Figure 5b, the average concentrations of the period 5-7 December exceed the legal threshold in all urban traffic and background stations, remaining below the limit only in CG (average concentration 29 $\mu g/m^3$).

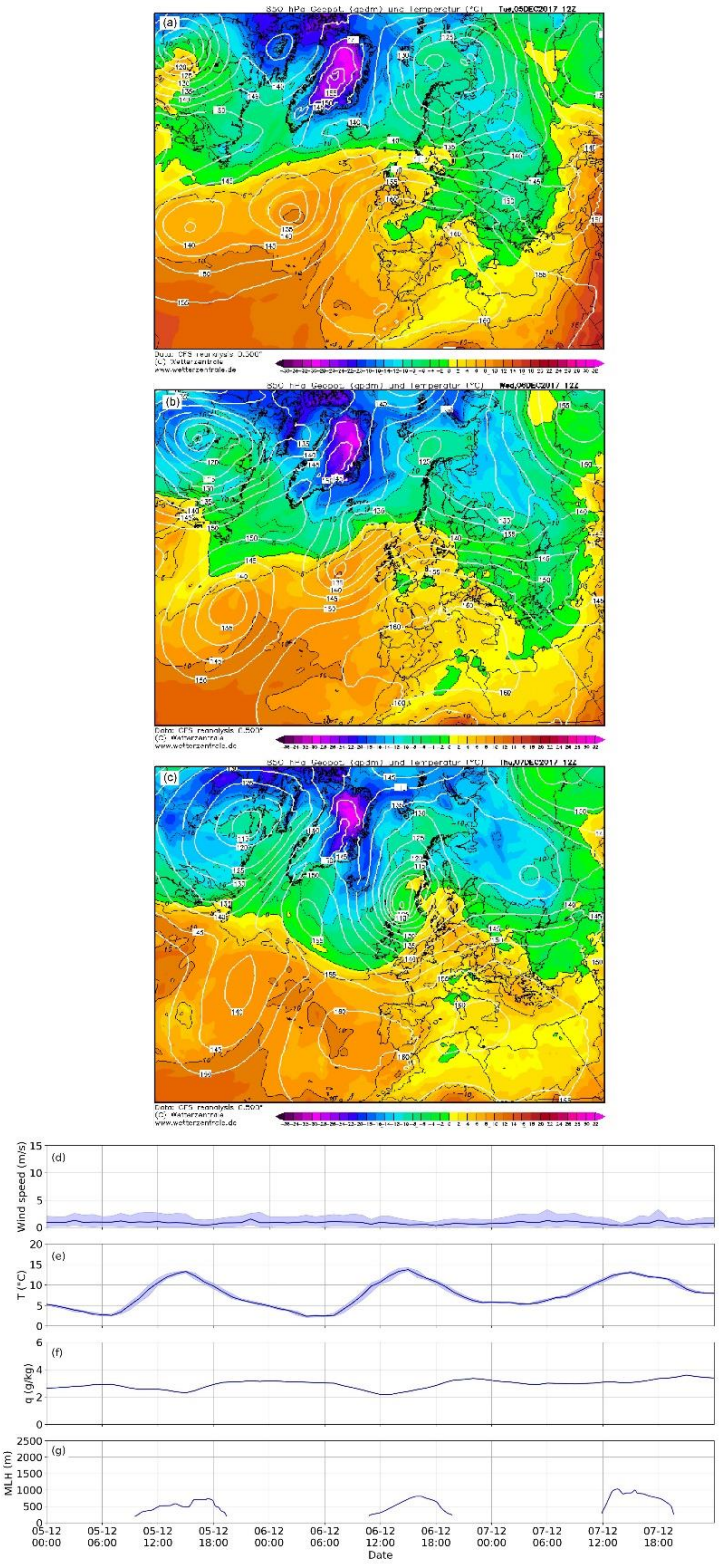

Figure 8. From (a) to (c): synoptic weather conditions from 5 to 7 December 2017 at 12:00 UTC from the Climate Forecast System (CFS) reanalysis. White contours refer to geopotential height at 850 hPa level (in geopotential decametres). Colours show air temperature (°C) at sea level (source: https://www.wetterzentrale.de/). Trends of: (d) wind speed, (e) air temperature, (f) specific humidity as a function of the time of day obtained by ground-based meteorological station at APL and (g) MLH from the ceilometer. Minimum and maximum values are depicted by filled areas around mean value lines.

The chemical composition of PM_{10} at APL station (Figure 5a) was characterised by a relevant contribution of the anthropogenic sources: traffic emission was responsible for 26% of the PM mass, while the contribution of nitrate was 11% (the mean values during the study period were 20% and 7%, respectively). A fast increase in the concentration of ammonium nitrate, which is originated by the reaction of nitric acid with ammonia, is generally observed in atmospheric stagnation conditions during the cold season, as it is enhanced by the high availability of NO_2 and by low temperature and high relative humidity. Nitrate concentration levels measured during these three days (5.3, 5.2, 5.6 $\mu g/m^3$, to be compared with a mean value of 1.9 $\mu g/m^3$ during the study period) are uncommonly high for this geographical area, where the conditions of strong atmospheric stability are generally of short duration. Higher values with respect to the mean concentration were also recorded for organics. Organics include a wide variety of components: some of them are emitted directly by the biosphere but many others are produced by the reaction of Volatile Organic Compounds (VOCs). As in the case of inorganic salts, this secondary production is enhanced during conditions of atmospheric stability. Soil and sea contributed less than average to PM composition. Since the wind blew from north and there was no breeze onset, also during this episode the contribution of the marine aerosols was very low (2%).

During this period, the AOD (Figure 9a) had two characteristic behaviours: until about 9:30 UTC on 5 December, it had a slightly increasing trend, ranging from 0.08 to 0.1. Then, it suddenly decreased, assuming values between 0.05 and 0.07. The AOD remained nearly constant on 6 December (around 0.055) and decreased again at 12:00 UTC. Unfortunately, there were no AOD observations on 7 December, as the cloudy sky did not allow direct sun measurements. Tropospheric NO_2 (Figure 9b) increased on 5 December, passing from 0.3 DU and 0.7 DU. On 6 December, the amount of tropospheric NO_2 oscillated between 0.2 DU and 0.55 DU. The measurements show low uncertainty, settling on approximately 0.05 DU. After 12:00 UTC on 7 December the content of tropospheric NO_2 significantly increased (as also the measurements error, that is around 0.25 DU), because of the irruption of the low-pressure center on Italy that determined a change in the direction (which comes from East, see Figure 3a) and an increase in the wind speed at the ground. Similarly, the near-surface NO_2 (Figure 9c) assumed almost constant values on 5 December (about 25 ppb). On 6 December, the near-surface amount of NO_2 increased until 12:00 UTC (35 ppb) when, in conjunction with the reduction of AOD and the growth of tropospheric NO_2, it began to decrease. On 7 December, it increased by almost 50% after 12:00 UTC (from 18 ppb to 30 ppb). The measurements uncertainty reaches 15-20 ppb, assuming lower values (about 2-5 ppb) only on the morning of 7 December. It is evident that the error increases as the measured concentration increases, especially when the value of 10 ppb is exceeded.

The analysis of this second event permits to conclude that, in the case of lasting thermal inversion, it is not easy to improve air quality because of the confinement of pollutants in the first layer of the atmosphere. Even if the winds are northerly, as in case study #1, the low velocities give rise to very different conditions: the synoptic weather conditions govern the development of the PBL and the consequent horizontal and vertical dispersion mechanisms. Results are in good agreement with Fortelli et al. (2016) who found in the coastal city of Naples (Italy) a close correlation between wind intensity, thermal inversion and high levels of PM in the atmosphere. Specifically, they found that the largest pollution periods usually occurred when the average daily wind speed was between 1 and 2 m/s. As a result, policy strategies should be planned and implemented in advance: during thermal inversion events, once the inversion has taken place, any emissive block could only decrease the slope of the increase in concentration but cannot lead to its decrease. It means that the air quality standards could be exceeded even if anthropogenic activities, such as transport and industries, are reduced thanks to specific strategies. Therefore, it is possible to decrease PM emissions by blocking traffic and anthropogenic activities, but it is essential to prevent

these situations: short- and medium-range weather forecasts are crucial for the prediction of thermal inversion episodes and, therefore, for the best design of mitigation strategies.

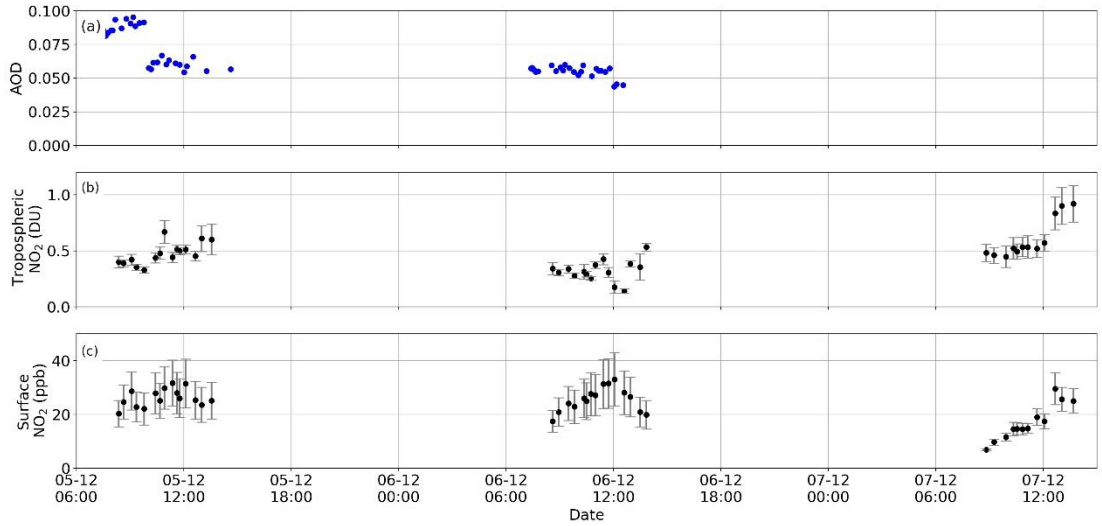

Figure 9. (a) Aerosol optical depth, (b) tropospheric and (c) near-surface amounts of NO_2 measured at APL station as a function of the time of day from 5 to 7 December 2017. Vertical bars depict measurement errors. Note the different vertical scale in panels (b) and (c) with respect to the other events.

4.3.Case study #3: 12 December 2017

During 12 December, the synoptic map (Figure 10a) shows, at 12:00 UTC, two low-geopotential height systems on the Scandinavian Peninsula and between Iceland and Greenland and a marked ridge on the Atlantic Ocean. In addition, anticyclonic pattern dominated the Mediterranean regions with weather conditions in Italy characterized by surface temperatures between 6 °C and 8 °C.

As recorded by SODAR (Figure 3a), from 00:00 UTC on 11 December, the high-geopotential heights system on the Mediterranean Basin caused South-easterly winds with velocity up to 9 m/s. During the afternoon of 12 December, the wind speed decreased and, in the evening, the direction changed too, settling on the South-West quadrant. Therefore, the event examined occurred in the terminal phase of an episode characterized by intense, southerly winds. The wind velocity decreased near the surface (Figure 10b) ranging from 6 m/s at 02:00 UTC down to 3 m/s after 22:00 UTC, i.e. when the wind direction changed due to the passive friction generated by the roughness of buildings and surface. During the night, wind gusts with speeds up to 13 m/s (at 5:00 UTC) were recorded. No thermal inversion is notable in the air temperature profiles collected at LIRE station (Figure 4, panels i and j). Surface air temperature (Figure 10c) assumed almost constant values (about 15 °C) throughout the day, well above the monthly average (8.2 °C in the period 1971-2000, source: http://clima.meteoam.it/AtlanteClimatico/ucf/%28235%29Roma%20Urbe.ucf). Note the absence of cooling during the night between 11 and 12 December, due to the presence of intense southerly winds and clouds, which maintained the temperature at about 15 °C during night-time. Specific humidity q (Figure 10d) was also nearly constant (4.1 g/kg) until 12:00 UTC, then it increased up to 5 g/kg at 21:00 UTC. Unfortunately, 12 December was a cloudy day and no MLH data was available.

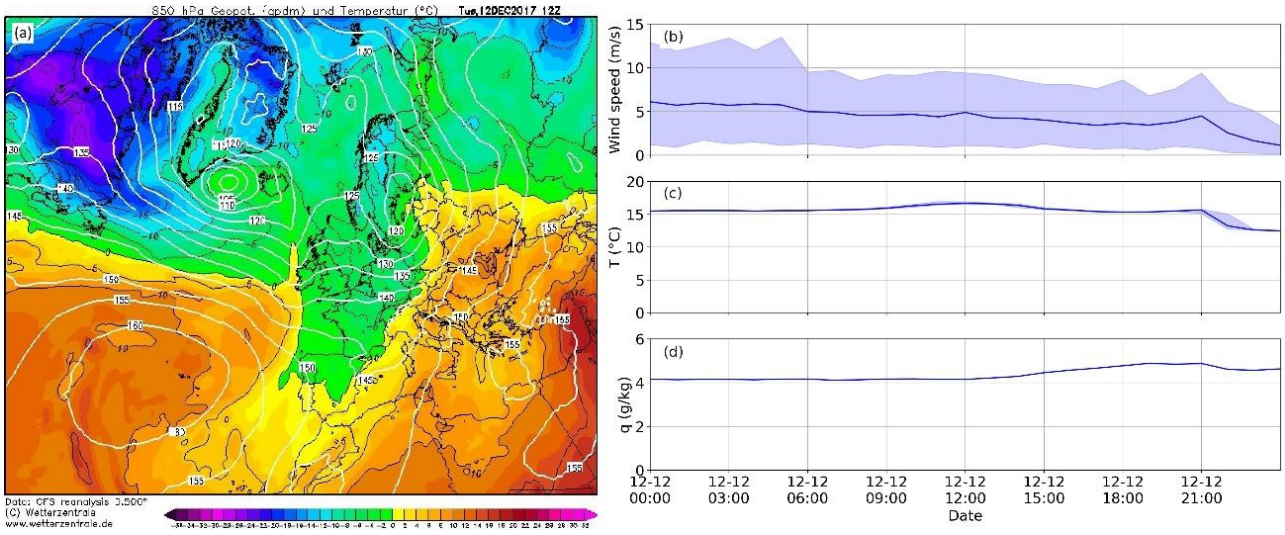

Figure 10. (a) Synoptic weather conditions on 12 December 2017 at 12:00 UTC from the Climate Forecast System (CFS) reanalysis. White contours refer to geopotential height at 850 hPa (in geopotential decametres). Colours show air temperature (°C) at sea level (source: https://www.wetterzentrale.de/). Trend of (b) wind speed, (c) air temperature and (d) specific humidity as a function of the time of day obtained by ground-based meteorological station in APL. Minimum and maximum values are depicted by filled regions.

Unlike the event of 5-7 December, on 12 December the concentration of PM_{10} increased (and decreased the following day) similarly in urban and rural stations, with values between 43 µg/m^3 (CG) and 70 µg/m^3 (MG). This trend was linked to large-scale aerosol transport phenomena, which affected the city and neighbouring areas in the same way and did not depend on local anthropogenic emissions. Results are in according with Gobbi et al. (2007) who analysed the role of Saharan dust advection in the exceeding of the PM_{10} thresholds in the city of Rome. They found an average impact of Saharan dust to daily PM_{10} of about 20 µg/m^3, with lower influence in the urban traffic stations, where the contribution by local emissions is relevant. The phenomenon lasted only one day: on 13 December, all stations registered particulate matter concentrations comparable to those of 11 December (minimum: 17 µg/m^3, CG; maximum: 27 µg/m^3, CI).

The HYSPLIT (Hybrid Single-Particle Lagrangian Integrated Trajectory) back trajectories from the READY system of the NOAA Air Resources Laboratory (ARL) (Draxler et al., 1998; Draxler et al., 2003) depicted in Figure 11, confirmed that the southerly winds (starting on 11 December) determined the advection of air masses coming from the Sahara Desert, which contained a high load of dust and marine aerosol. As expected, on 12 December, the crustal (21.8 µg/m^3) and marine (13.2 µg/m^3) components predominated the chemical composition of PM_{10}, with a total contribution of the two natural sources above 67%. The concentrations of organic aerosols (4.4 µg/m^3) and traffic emissions (2.6 µg/m^3) were quite low and close the values recorded during case study #1. Regarding secondary inorganics, the concentration of nitrate, 2.3 µg/m^3, was close to the mean value of the study period, while the concentration of sulphate was much higher (6.3 µg/m^3, to be compared to 1.2 µg/m^3). This remarkable sulphate concentration was likely due to the trajectories followed by the air masses: the concentration of SO_2, the gaseous precursor of particulate sulphate, is high both on the Mediterranean, due to the emission of vessels using heavy fuel oil, and in Northern Tunisia, due to industrial activity (Becagli et al., 2012).

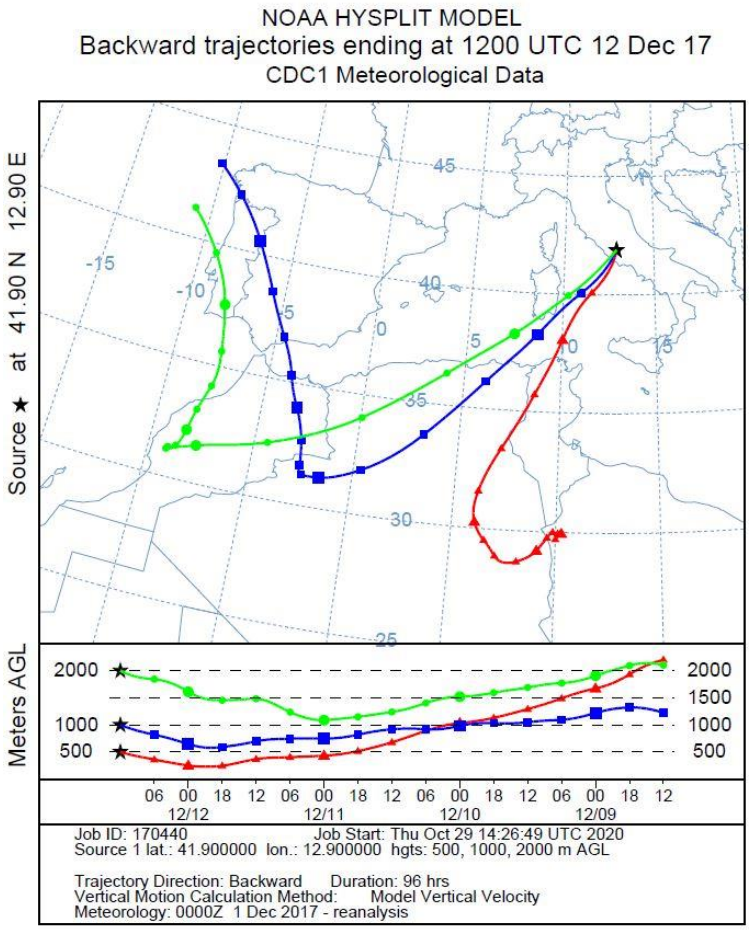

Figure 11. HYSPLIT 5-day back trajectories for 12 December 2017.

As the sky was cloudy, no AOD data about 12 December was available. Due to the lack of information, it is not possible to draw conclusions on the hourly variation of the aerosol composition. The tropospheric content of NO_2 (Figure 12a) did not vary during the day (about 0.2 DU). Only a slight increase (up to 0.25 DU) at 11:15 UTC and 13:40 UTC was notable even if, as shown by the error bars, the uncertainty related to these measures was the highest of the day (about 0.12 DU). The near-surface NO_2 (Figure 12b) assumed almost constant values during the day and was always below 10 ppb. The uncertainty of the measurements is around 1-3 ppb, i.e. comparable with what was seen in the case study #1.

The low levels of tropospheric and near-surface NO_2 underlined that the high PM_{10} concentrations recorded were not due to road traffic and anthropogenic sources but are mainly related to the long-range transport of dust and marine aerosols. Since the increase in particulate matter was not linked to local emissions, also in this case the adoption of measures apt to reduce atmospheric pollution levels can give limited results. Yet, as desert dust particles have been shown to also affect human health on both the short- and long-term, mitigation efforts on local emission in prediction of desert dust transport events should also be considered. This is even truer considering that during dust transport events high traffic levels can also play a role in enhancing dust resuspension (Barnaba et al., 2017).

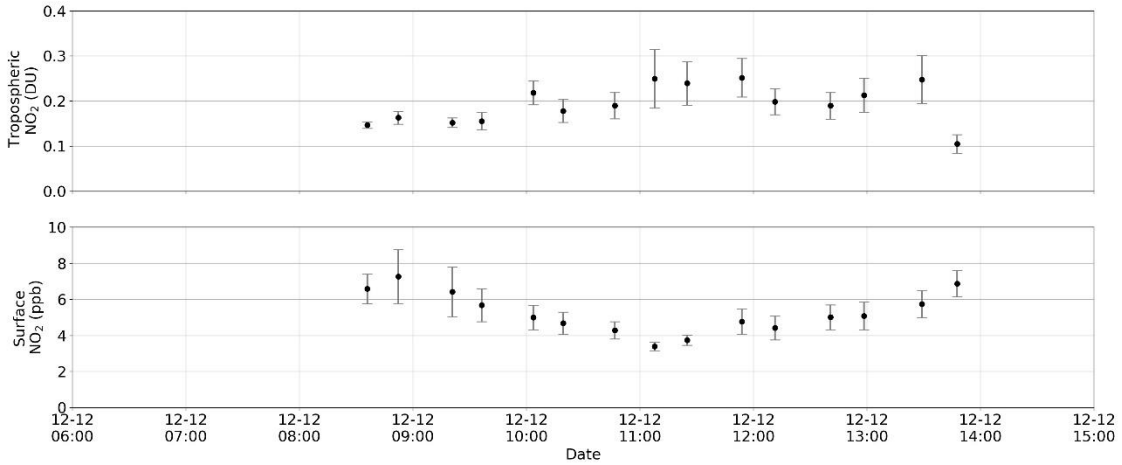

Figure 12. (a) Tropospheric and (b) near-surface amounts of NO_2 measured at APL station as a function of the time of day on 12 December 2017. Vertical bars depict measurement errors. Note the different vertical scale with respect to the other events.

5. Conclusions

During the winter of 2017, thanks to the in-situ campaign carried out in the framework of the VIEPI project, it was possible to have detailed information on concentration and chemical composition of PM_{10} in the urban area of Rome. In this work, three events are analysed to provide useful indications for the best planning of strategies for the air pollution reduction.

The salient findings of the study are summarized below:

(i) Excluding rainy conditions, the "optimal" case, in terms of air quality and ventilation, occurs in the case of northerly, synoptic winds with wind velocity greater than 4 m/s persisting for at least 24 hours. The cold, dry continental air "cleans" the PBL, favouring the pollutants dispersion. In this case, the PM_{10} concentrations both in urban and rural stations were similar and below 15 $\mu g/m^3$.

(ii) In the case of continuous thermal inversion and low speed winds, the horizontal and vertical dispersion is very limited, causing the accumulation of pollutants near the ground and the consequent increase of PM_{10} concentration in urban area. The adopted measures of temporary limitations of road traffic and anthropogenic activities could only decrease the slope of the increase in concentration but cannot lead to its decrease. In order to avoid the trapping of pollutants in the inversion layer and to optimize the efficiency of such measures, it is essential to exploit weather forecasts and schedule road traffic blocks before the thermal inversion occurs. Anyway, only the change in weather conditions and the disappearance of the thermal inversion layer can substantially improve air quality.

(iii) In the investigated area, the increase in PM_{10} concentration can also be due to the advection of air masses with a high load of Saharan dust and marine aerosol. In this case, it would be beneficial to mitigate local emissions in prediction of significant desert dust transport events, although, also in these cases, only the change in synoptic circulation can substantially improve air quality.

In light of these considerations, it is evident that the implementation of a short- and medium-term forecasting service both for weather and air quality conditions, capable of providing information to the government, could be vital in defining guidelines for the correct planning of air quality improvement strategies. Moreover, the combination of meteorological and air quality numerical models with high-resolution domains could be useful for the evaluation of pollutant loads within the urban area, considering parameters such as daily evolution of MLH, friction velocity as well as wind speed, wind direction and hydrometric data, in order to exhaustive investigate the PBL.

Funding: This research was supported by INAIL in the frame of its scientific research programs (2016-2018) and by BAQUNIN Project team, funded by ESA through the contract ID 4000126749/19/I-NS.

Acknowledgments: The authors gratefully acknowledge the BAQUNIN team for the support and the atmospheric data, ARPA Lazio for providing particulate matter measurements, Fondazione Osservatorio Milano Duomo for the meteorological data and Italian Air Force Meteorological Service/World Meteorological Organization for radiosoundings used in this work. The Pandonia Global Network (PGN) is a bilateral project supported with funding from NASA and ESA. We are also grateful to Alexander Cede and Martin Tiefengraber for having kindly provided the NO_2 data from PGN, to Enrico Cadau for the careful analysis of the PBL and to Roberto Salzano for his precious scientific comments and discussions.

References

Avino, P., De Lisio, V., Grassi, M., Lucchetta, M.C., Messina, B., Monaco, G., Petraccia, L., Quartieri, G., Rosentzwin R., Russo, M.V., Spada, S., Valenzi, V.I. 2004. Influence of air pollution on chronic obstructive respiratory diseases: comparison between city (Rome) and hillcountry environments and climates. Annali di Chimica: Journal of Analytical, Environmental and Cultural Heritage Chemistry, 94(9-10), 629-636. DOI: 10.1002/adic.200490080

Baltaci, H., Alemdar, C.S.O., Akkoyunlu, B.O. 2020. Background atmospheric conditions of high PM10 concentrations in Istanbul, Turkey. Atmos. Pollut. Res., 11(9), 1524-1534. DOI: 10.1016/j.apr.2020.06.020

Barbano, F., Brattich, E., Di Sabatino, S.2020. Characteristic Scales for Turbulent Exchange Processes in a Real Urban Canopy. Bound.-Layer Meteorol., 1-24. DOI: 10.1007/s10546-020-00554-5

Barnaba, F., Angelini, F., Curci, G., Gobbi, G.P. 2011. An important fingerprint of wildfires on the European aerosol load. Atmos. Chem. Phys., 11, 10487-10501. DOI: 10.5194/acp-11-10487-2011

Barnaba, F., Bolignano, A., Di Liberto, L., Morelli, M., Lucarelli, F., Nava, S., Perrino, C., Canepari, S., Basart, S., Costabile, F., Dionisi, D. 2017. Desert dust contribution to PM10 loads in Italy: Methods and recommendations addressing the relevant European Commission Guidelines in support to the Air Quality Directive 2008/50. Atmos. Environ., 161, 288-305. DOI: 10.1016/j.atmosenv.2017.04.038

Becagli, S., Sferlazzo, D.M., Pace, G., Di Sarra, A., Bommarito, C., Calzolai, G., Lucarelli, F., Meloni, D., Monteleone, F., Severi, M., Traversi, R., Udisti, R., 2012. Evidence for heavy fuel oil combustion aerosols from chemical analyses at the island of Lampedusa: a possible large role of ships emissions in the Mediterranean. Atmospheric Chemistry and Physics, 12(7), 3479. DOI: 10.5194/acp-12-3479-2012.

Campanelli M., Iannarelli A.M., Mevi G., Casadio S., Diémoz H., Finardi S., Dinoi A., Castelli E., diSarra A., Di Bernardino A., Casasanta G., Bassani C., Cadau E., Siani A.M., Cacciani M., Barnaba F., Di Liberto L., Argentini S. 2021. Atmospheric Examination at some italian Regional capitals during the emergency LOckdown for Covid-19 Using a Synergistic network of measurements (AER LOCUS), manuscript submitted

Campanelli, M., Siani, A. M., di Sarra, A., Iannarelli, A. M., Sanò, P., Diémoz, H., Casasanta, G., Cacciani, M., Tofful, L., Dietrich, S. 2019. Aerosol optical characteristics in the urban area of Rome, Italy, and their impact on the UV index. Atmos. Meas. Tech. Discuss., 1-23.

Cantelli, A., Monti, P., Leuzzi, G. 2015. Numerical study of the urban geometrical representation impact in a surface energy budget model. Environ. Fluid Mech., 15(2), 251-273. DOI: 10.1007/s10652-013-9309-0

Casasanta, G., Di Bernardino, A., Iannarelli, A.M., Casadio, S., Petenko, I., Argentini, S., Mevi, G., Cacciani, M. 2020. Estimating the accuracy in vertical wind speed determination with Doppler SODAR, manuscript in preparation.

Cattani, G., di Bucchianico, A.D.M., Dina, D., Inglessis, M., Notaro, C., Settimo, G., Viviano, G., Marconi, A. 2010. Evaluation of the temporal variation of air quality in Rome, Italy from 1999 to 2008. Annali dell'Istituto superiore di sanità, 46, 242-253. DOI: 2010.v46n3/242-253/

Cede, A. 2019. Manual for Blick Software Suite 1.7, LUFTBLICK Earth Observation Technologies.

Cede, A., Tiefengraber, M., Gebetsberger, M., Kreuter, A. 2019. Fiducial Reference Measurements for Air Quality, LuftBlick Report 201909, Earth Observation Technologies.

Cenedese, A., Miozzi, M., Monti, P. 2000. A laboratory investigation of land and sea breeze regimes. Exp. Fluids, 29(1), S291-S299. DOI: 10.1007%2Fs003480070031

Chester, R., Sharples, E. J., Sanders, G. S., Saydam, A. C. 1984. Saharan dust incursion over the Tyrrhenian Sea. Atmos. Environ., 18(5), 929-935. DOI: 10.1016/0004-6981(84)90069-6

Ciardini, V., Di Iorio, T., Di Liberto, L., Tirelli, C., Casasanta, G., di Sarra, A., Fiocco, G., Fuà, D., Cacciani, M. 2012. Seasonal variability of tropospheric aerosols in Rome. Atmos. Res., 118, 205-214. DOI: 10.1016/j.atmosres.2012.06.026

Davis, L.W. 2008. The effect of driving restrictions on air quality in Mexico City. J. Political Econ., 116(1), 38-81. DOI: 10.1086/529398

Di Bernardino, A., Iannarelli, A.M., Casadio, S., Mevi, G., Campanelli, M., Casasanta, G., Cede, A., Tiefengraber, M., Siani, A.M., Cacciani, M. 2020. On the effect of sea breeze regime on optical and physical aerosol properties in the urban area of Rome, Italy, Urban Clim., manuscript submitted

Di Bernardino, A., Monti, P., Leuzzi, G., Querzoli, G. 2018. Pollutant fluxes in two-dimensional street canyons. Urban climate, 24, 80-93. DOI: 10.1016/j.uclim.2018.02.002

Dionisi, D., Barnaba, F., Diémoz, H., Di Liberto, L., Gobbi, G.P., 2018. A multiwavelength numerical model in support of quantitative retrievals of aerosol properties from automated lidar ceilometers and test applications for AOT and PM 10 estimation. Atmos. Meas. Tech., 11(11), p.6013. DOI: 10.5194/amt-11-6013-2018

Draxler, R.R., Hess, G.D., 1998. An overview of the HYSPLIT-4 modeling system for trajectories, dispersion and deposition. Aust. Meteorol. Mag., 47, 295–308.

Draxler, R.R., Rolph, G.D. 2003. 'HYSPLIT – (Hybrid, Single-Particle Lagrangian Integrated Trajectory): Model access via NOAA ARL READY' /http://www.arl.noaa.gov/ready/hysplit4.htmlS., NOAA Air Resources Laboratory, Silver Spring, MD

Elminir, H. K. 2005. Dependence of urban air pollutants on meteorology. Sci. Total Environ., 350(1-3), 225-237. DOI: 10.1016/j.scitotenv.2005.01.043

EU. 1999. Council Directive 1999/30/EC of 22 April 1999 relating to limit values for sulphur dioxide, nitrogen dioxide and oxides of nitrogen, particulate matter and lead in ambient air. Official Journal of the European Union, L163 (29/06/1999), 41–60.

EU. 2008. Directive 2008/50/EC of the European Parliament and of the Council of 21 May 2008 on ambient air quality and cleaner air for Europe, Official Journal of the European Union, L152 (11/06/2008), 1-44.

Farao, C., Canepari, S., Perrino, C., Harrison, R.M. 2014. Sources of PM in an Industrial Area: Comparison between receptor model Results and semiempirical calculations of source contributions. Aerosol Air Qual. Res., 14, 1558–1572. DOI: 10.4209/aaqr.2013.08.0281

Fortelli, A., Scafetta, N., & Mazzarella, A. 2016. Influence of synoptic and local atmospheric patterns on PM10 air pollution levels: a model application to Naples (Italy). Atmos. Environ., 143, 218-228. DOI: 10.1016/j.atmosenv.2016.08.050

Giles, D.M., Sinyuk, A., Sorokin, M.G., Schafer, J.S., Smirnov, A., Slutsker, I., Eck., T.F., Holben, B.N., Lewis, J.R., Campbell, J.R., Welton, E.J., Korkin, S.V., Lyapustin, A.I. 2017. Advancements in the Aerosol Robotic Network (AERONET) Version 3 database–automated near-real-time quality control algorithm with improved cloud screening for Sun photometer aerosol optical depth (AOD) measurements. Atmos. Meas. Tech., 12(1). DOI: 10.5194/amt-12-169-2019

Gobbi, G. P., Barnaba, F., Ammannato, L. 2007. Estimating the impact of Saharan dust on the year 2001 PM10 record of Rome, Italy. Atmos. Environ., 41(2), 261-275. DOI: 10.1016/j.atmosenv.2006.08.036

Gobbi, G. P., Barnaba, F., Di Liberto, L., Bolignano, A., Lucarelli, F., Nava, S., Perrino, C., Pietrodangelo, A., Basart, S., Costabile, F., Dionisi, D., Rizza, U., Canepari, S., Sozzi, R., Morelli, M., Manigrasso, M., Drewnick, F., Struckmeier, C., Poenitz, K., Wille, H. 2019. An inclusive view of Saharan dust advections to Italy and the Central Mediterranean. Atmos. Environ., 201, 242-256. DOI: 10.1016/j.atmosenv.2019.01.002

Haeffelin, M., Angelini, F., Morille, Y., Martucci, G., Frey, S., Gobbi, G.P., Lolli, S., O'dowd, C.D., Sauvage, L., Xueref-Rémy, I., Wastine, B. 2012. Evaluation of mixing-height retrievals from automatic profiling lidars and ceilometers in view of future integrated networks in Europe. Bound.-Layer Meteorol., 143(1), 49-75. DOI: 10.1007/s10546-011-9643-z

Hart, J. E., Yanosky, J. D., Puett, R. C., Ryan, L., Dockery, D. W., Smith, T. J., Garshick, E., Laden, F. 2009. Spatial modeling of PM10 and NO2 in the continental United States, 1985–2000. Environmental health perspectives, 117(11), 1690-1696. DOI: 10.1289/ehp.0900840

Hassan, H., Latif, M.T., Juneng, L., Amil, N., Khan, M.F., Yik, D.J., Abdullah, N.A. 2020. Interaction of PM10 concentrations with local and synoptic meteorological conditions at different temporal scales. Atmos. Res., 104975. DOI: 10.1016/j.atmosres.2020.104975

He, G.X., Yu, C.W.F., Lu, C., Deng, Q.H. 2013. The influence of synoptic pattern and atmospheric boundary layer on PM10 and urban heat island. Indoor Built Environ. 22(5), 796-807. DOI: 10.1177/1420326X13503576

Heinrich, J., Thiering, E., Rzehak, P., Krämer, U., Hochadel, M., Rauchfuss, K. M., Gehring, U., Wichmann, H.-E. 2013. Long-term exposure to NO2 and PM10 and all-cause and cause-specific mortality in a prospective cohort of women. Occup. Environ. Med., 70(3), 179-186. DOI: 10.1136/oemed-2012-100876

Jayaratne, E.R., Clifford, S., Morawska, L. 2015. Atmospheric visibility and PM10 as indicators of new particle formation in an urban environment. Environ. Sci. Technol., 49(21), 12751-12757. DOI: 10.1021/acs.est.5b01851

Ji, D.S., Wang, Y.S., Wang, L.L., Chen, L.F., Hu, B., Tang, G.Q., Xin, J., Song, T., Wen, T., Sun, Y., Pan, Y., Liu, Z. 2012. Analysis of heavy pollution episodes in selected cities of northern China. Atmos. Environ. , 50, 338–348. DOI: 10.1016/j.atmosenv.2011.11.053

Kim, K.H., Kabir, E., Kabir, S. 2015. A review on the human health impact of airborne particulate matter. Environ. Int., 74, 136-143. DOI: 10.1016/j.envint.2014.10.005

Li, Z., Guo, J., Ding, A., Liao, H., Liu, J., Sun, Y., Wang, T., Xue, H., Zhang, H., Zhu, B. 2017. Aerosol and boundary-layer interactions and impact on air quality. Natl. Sci. Rev. 4(6), 810-833. DOI: 10.1093/nsr/nwx117

Macias, E.S., Husar, R.B. 1976. Atmospheric particulate mass measurement with beta attenuation mass monitor. Environ. Sci. Technol., 10(9), 904-907.

Martin-Vide, J., Sarricolea, P., Moreno-García, M. C. 2015. On the definition of urban heat island intensity: the "rural" reference. Front. Earth Sci., 3, 24. DOI: 10.3389/feart.2015.00024

Mastrantonio, G., Fiocco, G. 1982. Accuracy of wind velocity determinations with Doppler sodars. J. Appl. Meteorol., 21(6), 823-830. DOI: 10.1175/1520-0450(1982)021<0823:AOWVDW>2.0.CO;2

Mevi, G., Casadio, S., Iannarelli, A.M., Campanelli, M., Di Bernardino, A., Bassani, C., Cacciani, M., Siani, A.M., Cede, A., Tiefengraber, M., von Bismark, J., Dehn, A. 2021. Impact of lock-down measures on NO2 concentration in Rome as observed in two BAQUNIN sites, Aerosol Air Qual. Res., manuscript submitted

Michelozzi, P., Forastiere, F., Perucci, C.A., Fusco, D., Barca, A., Spadea, T. 2000. Acute effects of air pollution in Rome. Annali dell'Istituto superiore di sanità, 36(3), 297-304.

Oke, T. R. 1973. City size and the urban heat island. Atmos. Environ. (1967), 7(8), 769-779. DOI: 10.1016/0004-6981(73)90140-6

Olofson, K.F.G., Andersson, P.U., Hallquist, M., Ljungström, E., Tang, L., Chen, D., Pettersson, J.B. 2009. Urban aerosol evolution and particle formation during wintertime temperature inversions. Atmos. Environ. , 43(2), 340-346. DOI: 10.1016/j.atmosenv.2008.09.080

Palmieri, S., Durante, G., Siani, A. M., Casale, G. R. 2008. Atmospheric stagnation episodes and hospital admissions. Public health, 122(10), 1128-1130. DOI: 10.1016/j.puhe.2008.02.006

Pelliccioni, P., Monti, P., Cattani, G., Boccuni, F., Cacciani, M., Canepari, M., Capone, P., Catambrone, M., Cusano, M., D'Ovidio, M.C., De Santis, A., Di Bernardino, A., di Bucchianico, A.D.M., Di Renzi, S., Ferrante, R., Gaeta, A., Gaddi, R., Gherardi, M., Giusto, M., Gordiani, A., Grandoni, L., Leone, G., Leuzzi, G., L'Episcopo, N., Marcovecchio, F., Pini, A., Sargolini T., Tombolini, F., Tofful, L., Perrino, C. 2020. Integrated evaluation of indoor particulate exposure: the VIEPI project. Sustainability, 12, 9758. DOI:10.3390/su12229758

Perrino, C., Canepari, S., Catrambone, M., Dalla Torre, S., Rantica, E., Sargolini, T. 2009. Influence of natural events on the concentration and composition of atmospheric particulate matter. Atmos. Environ., 43(31), 4766-4779. DOI: 10.1016/j.atmosenv.2008.06.035

Perrino, C., Catrambone, M., Pietrodangelo, A. 2008. Influence of atmospheric stability on the mass concentration and chemical composition of atmospheric particles: a case study in Rome, Italy. Environ. Iintern., 34(5), 621-628. DOI: 10.1016/j.envint.2007.12.006

Perrino, C., Tofful, L., Dalla Torre, S., Sargolini, T., Canepari, S. 2019. Biomass burning contribution to PM10 concentration in Rome (Italy): Seasonal, daily and two-hourly variations. Chemosphere, 222, 839-848. DOI: 10.1016/j.chemosphere.2019.02.019

Petenko, I., Mastrantonio, G., Viola, A., Argentini, S., Coniglio, L., Monti, P., Leuzzi, G. 2011. Local circulation diurnal patterns and their relationship with large-scale flows in a coastal area of the Tyrrhenian Sea. Bound.-layer Meteorol. 139(2), 353-366. DOI: 10.1007/s10546-010-9577-x

Pey, J., Querol, X., Alastuey, A., Forastiere, F., Stafoggia, M. 2013. African dust outbreaks over the Mediterranean Basin during 2001-2011: PM10 concentrations, phenomenology and trends, and its relation with synoptic and mesoscale meteorology. Atmos. Chem. Phys., 13(3), 1395. DOI: 1 0.5194/acp-13-1395-2013

Pope, III C.A., Burnett, R.T., Thun, M.J., Calle, E.E., Krewski, D., Ito, K., Thurston, G. D. 2002. Lung cancer, cardiopulmonary mortality, and long-term exposure to fine particulate air pollution. Jama., 287(9), 1132-1141. DOI: 10.1001/jama.287.9.1132

Rojas, A.L.P., Borge, R., Mazzeo, N.A., Saurral, R.I., Matarazzo, B.N., Cordero, J.M., Kropff, E. 2020. High PM10 concentrations in the city of Buenos Aires and their relationship with meteorological conditions. Atmos. Environ., 241, 117773. DOI: 10.1016/j.atmosenv.2020.117773

Sinyuk, A., Holben, B.N., Eck, T.F., Giles, D.M., Slutsker, I., Korkin, S., Schafer, J.S., Smirnov, A., Sorokin, M., Lyapustin, A. 2020. The AERONET Version 3 aerosol retrieval algorithm, associated uncertainties and comparisons to Version 2. Atmos. Meas. Techn., 13(6), 3375-3411. DOI: 10.5194/amt-13-3375-2020

Spinei, E., Tiefengraber, M., Müller, M., Cede, A., Berkhout, S., Dong, Y., Nowak, N. 2020. Simple retrieval of atmospheric trace gas vertical concentration profiles from multi-axis DOAS observations, manuscript in preparation.

Stull R.B. 1988. An Introduction to Boundary-layer Meteorology. Kluwer Acad. Publ., Dordrecht-Boston-London, 666.

Su, T., Li, Z., Kahn, R. 2018. Relationships between the planetary boundary layer height and surface pollutants derived from lidar observations over China: regional pattern and influencing factors. Atmos. Chem. Phys., 18(21). DOI: 10.5194/acp-18-203-2018

Tetens, O. 1930. Uber cinige meteorologische Begriffe. Zeitschrift fur Geophysik, 6, 297–309. Friedrich Vieweg & Sohn Akt. Gesellschaft.

Triantafyllou, A. G. 2001. PM10 pollution episodes as a function of synoptic climatology in a mountainous industrial area. Environ. Pollut., 112(3), 491-500. DOI: 10.1016/S0269-7491(00)00131-7

Viard, V.B., Fu, S. 2015. The effect of Beijing's driving restrictions on pollution and economic activity. J. Public Econ., 125, 98-115. DOI: 10.1016/j.jpubeco.2015.02.003

Weinmayr, G., Romeo, E., De Sario, M., Weiland, S. K., Forastiere, F. 2010. Short-term effects of PM10 and NO2 on respiratory health among children with asthma or asthma-like symptoms: a systematic review and meta-analysis. Environ. Health Perspect., 118(4), 449-457. DOI: 10.1289/ehp.0900844

World Health Organization. 2000. Air quality guidelines for Europe.

Zhao, D., Xin, J., Gong, C., Quan, J., Wang, Y., Tang, G., Ma, Y., Dai, L., Wu, X., Liu, G., Ma, Y. 2020. The impact threshold of the aerosol radiation forcing on the boundary layer structure in the pollution region. Atmos. Chem. Phys., 1-32. DOI: 10.5194/acp-2020-553